# Molecular BioSystems

Accepted Manuscript


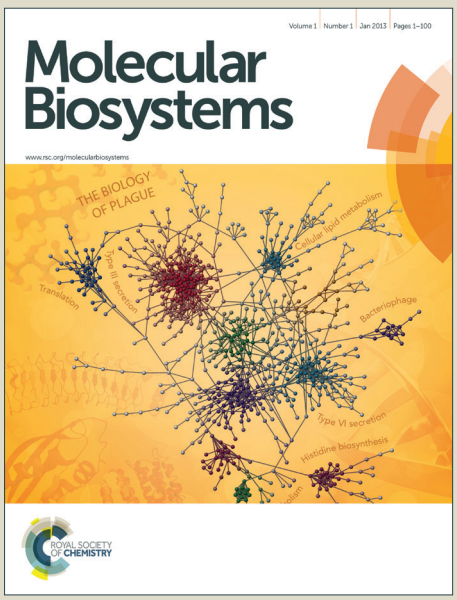





ROYAL SOCIETY OF CHEMISTRY

www.rsc.org/molecularbiosystems

# *Molecular BioSystems*

**Research interfacing chemical biology with the -omic sciences and systems biology**


**MISSION**: To stimulate and publish cutting-edge research interfacing chemical biology, systems biology and the omic sciences

Encouraging interdisciplinary work concerned with, in particular (but not limited to) cellular processes, metabolism, proteomics and genomics, systems biology, drug discovery, biomaterials and technologies/methodologies relevant to these subjects

**Please consider these standards when making your decision to accept or reject**

## Guidelines to Referees

**It is essential that all articles submitted to *Molecular BioSystems* meet novelty criteria for the journal; lack of novelty is sufficient reason for rejection**

**Routine work**, no matter how competently executed, should **not** be recommended for publication

**Methods** should report useful new methodology; the advantages of the reported work must be clearly presented, for example by comparison with established procedures.

**Communications** must contain novel research of such significance and/or interest as to warrant rapid publication; they should not be short papers.

*When preparing your report, please:*

- comment on the originality, importance, impact and scientific reliability of the work;
- state unequivocally whether you would like to see the paper accepted or rejected and give detailed comments (with references, as appropriate) that will both help the Editor to make a decision on the paper and the authors to improve it;
- do not make comments about the manuscript or authors which may cause offence.

*When submitting your report, please:*

- provide your report rapidly and within the specified deadline, or inform the Editor immediately if you cannot do so;
- submit your report at www.rsc.org/referees

**The online service for RSC authors and referees can be found at http://mc.manuscriptcentral.com/rsc**

**For further information about *Molecular Biosystems*, please visit: http://pubs.rsc.org/en/Journals/JournalIssues/MB**

**Responses to Comments**

Here we are giving one by one response to the comments raised by respected reviewers. Undoubtably, valuable comments given by the reviewer are really very useful to elevate the scientific standard of this article.

- **To provide.....such confusions.**

  As per comments given by reviewer error bars are incorporated in the figure 8 as well as values are now listed in table 2. We are also agree with the reviewer with the fact that DLS is very sensitive to minor population and we also got the high molecular weight aggregates but the % intensity of these species was found to be below 10 % that may be considered not significant with compare to monomer species which have high intensities and low polydispersity (<15%). Keeping reviewer's suggestions in mind we add the Rh distribution in tables moreover, we also given the supplementary files of DLS separately as directly given by DLS with proper % intensities, Rh distribution. Rh is of course stands for hydrodynamic radius, but DLS instrument used in this experiments (Wyatt technology) also give the results in the form of diameter so previously we represented our results in the form of diameter. Although reviewers statement is more appropriate that we should represent hydration in the form of Rh so here in revised manuscript we present the diameter values as Rh.

- **In the 3D fluoresence.....changes.**

  Peak 2 mainly reflects the spectral behaviour of Trp which is mainly caused by the transition of n→Π* of aromatic amino acids in BSA. Peak 3 exhibits the spectral characteristics of the polypeptide backbone ( Π→Π* transition ) as reported in the article. Reviewer stated peak 2 and 3 have close intensities but in actual it is not so. In table 3 for BSA limonene system, peak 2 intensity decreases from 333.5→313.2 nm and peak 3 from 261.2→252.9 nm is clearly indicated the BSA was quenched in the presence of limonene and further confirmed the binding of limonene to BSA. Moreover, quenching of BSA to limonene is concentration dependent as described by fluorescence quenching experiment. This alteration in peak intensity is significant enough because measurement was observed at the first titration condition mean ratio of BSA to limonene was kept 1:1 as reported earlier in our article (Ishtikhar M, Badr G, Osama A, Khan RH, Mol. Biosys,

2014 (10.1039/C4MB00306C). We also labelled intensity with peak in table 3 to avoid confusion.

- **To validate.....interactions.**

  Sudlow site 1 (Lys-197 to Glu 291) located in subdomain II A (Leu 176 to Lys 204) with part of six α helices from h1-h6. Specific residues present in Site I are h1 (Lys 197), h2 (Phe 210, Trp 213, Ala 214, Arg 217, Leu 218, Arg 217, Leu 218, Phe 222), h3 ( Leu 233, Leu 237, His 241), h4 (Arg 256, Leu 259, Ala 260, Ile 263), h6 ( Ile 289, Ala 290) as given in T. Peters Jr All about albumin: biochemistry, genetics, and medical applications, Academic press, 1995. Warfarin is well known site I marker for both BSA as well as HSA as reported earlier (J. Tian, J. Liu, Z. Hu and X. Chen, Bioorganic & Medicinal Chemistry, 2005, 13, 4124-4129, Y. Song, Y. Liu, W. Liu, F. A. Villamena and J. L. Zweier, RSC Advances, 2014, 4, 47649-47656.). Warfarin complex with albumin involves the residue present in the domain I as described in M. Dockal, M. Chang, D. C. Carter, Uuml and F. Ker, PRS, 2000, 9, 1455-1465. Molecular docking study of BSA-limonene depicted the amino acid residues involved i.e., Tyr149, Arg217, Leu237, Arg256, Leu259, Ala260, Ile263, Ser286, Ile289, and Ala290. So as described above most of the amino acids from Site I and all from domain I. In the last, we can say the both warfarin and limonene shares same site on BSA i.e., Site I on subdomain IIA so warfarin is the appropriate site marker for site I. Displacement study and docking study are well supported to depict the site I as limonene binding site on BSA. (Zhang X, Li L, Xu Z, Liang Z, Su J, et al. (2013). PLoS ONE 8(3): e59106. doi:10.1371/journal.pone.0059106. Hossain M, Khan AY, Suresh Kumar G (2011). PLoS ONE 6(4): e18333. doi:10.1371/journal.pone.0018333)

- Resolution.....factor.

  Resolution of right panel figure 10B is increased to 600dpi as per journal requrement.

- The abbreviation of WAR.....specified.

  Short forms WAR and DIA are replaced with full form i.e., warfarin and diazepam.

  All grammatical mistakes are corrected and manuscript is further fully checked before resubmission.

Research article

# Elucidating the Interaction of Limonene with Bovine Serum Albumin: A Multi-technique Approach

Sumit Kumar Chaturvedi, Ejaz Ahmad, Javed Masood Khan, Parvez Alam, Mohd Ishtikhar and Rizwan Hasan Khan*

*Interdisciplinary Biotechnology Unit, Aligarh Muslim University, Aligarh 202002, India*

*** To whom correspondence should be addressed:**

**Tel.: +91 571 2720388;**
**Fax: +91 571 2721776;**
**E-mail:** rizwanhkhan1@gmail.com
rizwanhkhan1@yahoo.com

## Abstract

The interaction of Bovine Serum Albumin (BSA) to limonene has been studied by UV-visible spectroscopy, fluorescence spectroscopy and molecular docking whereas its effects on protein conformation, topology and stability were determined by Circular Dichroism (CD), Dynamic Light Scattering (DLS) and Differential Scanning Calorimetry (DSC). A gradual decrease in Stern-Volmer quenching constants with the increase in temperature showed static mode of fluorescence quenching. The obtained binding constant ($K_b$) was ~$10^4$ $M^{-1}$. The temperature dependent $K_b$, Gibbs free energy ($\Delta G$), enthalpy ($\Delta H$) and entropy ($\Delta S$) changes were calculated which revealed that reaction is spontaneous and exothermic. The UV-visible spectra showed change in the peaks within aromatic region indicated hydrophobic interactions with Trp, Tyr and Phe in the protein. Moreover, limonene induced increase in α-helical contents probably on the cost of random coils or/and ß-sheets of BSA as observed from far-UV CD spectra. The topology of BSA in the presence of limonene was slightly altered as obtained from DLS results. The stability was also enhanced as revealed through thermal denaturation study by DSC and CD. Molecular docking study depicted limonene fits into the hydrophobic pocket close to Sudlow site I in domain IIA of BSA. The present study will be helpful to understand the binding mechanism of limonene and associated stability and conformational changes.


**Key words:** BSA; limonene; binding; CD; DSC; molecular docking.

## *1. Introduction*

Plant derived products have always been preferred over commercial ones for medicinal purpose. Flavonoids, polyphenols and medicinal products are extensively used for antioxidant, anti-inflammatory, anticancer, antimicrobial, antidermatophytic and hepatoprotective activities [1, 2]. Serum albumins are the most abundant proteins in the circulatory system of the wide variety of organisms which play dominant key role in binding and transport of numerous endogenous and exogenous ligands [3]. Serum albumin often enhances the apparent solubility of hydrophobic drugs in plasma and modulates their delivery, disposition, efficacy and distribution to cells in vivo and in vitro [4, 5]. The drug–protein interaction may result in the formation of a stable protein–drug complex, which has significant effect on the delivery, distribution, free concentration and the metabolism of drugs in the blood circulatory system. Thus, the drug–albumin complex may be considered as a model to gain fundamental insights into drug–protein interactions and explores its applications. In this study, BSA has been chosen because of its structural homology with human serum albumin (HSA), low cost, easy availability and unusual ligand-binding properties [6-10].

BSA is a non glycated and globular protein composed of 583 amino acids. It is made up of three homologous domains (I, II, III), which are separated into nine loops (L1–L9) by 17 disulphide bridges [11]. The loops in each domain are designed of a sequence of large–small–large loops forming a triplet. Each domain in turn is the resultant of two subdomains. BSA has two tryptophan, Trp-134 and Trp-212 which are embedded in the sub domain IB and sub domain IIA respectively [12, 13].

The molecular interactions among proteins and many compounds such as drugs and some organic small molecules have been investigated successfully [14-21]. However, the binding of plant derived products to serum albumins are now an emerging field to explore the role of plant derivatives in biological systems of herbivores and their mode of action in various diseases [22, 23].

Limonene exists as two optical isomers, *d*- and *l*-limonene, and the racemic mixture dipentene. Limonene, like other monoterpenes, occurs naturally in certain trees, bushes mainly in peel from citrus fruits, in dill, caraway, fennel, turpentine and in celery. Limonene is used as a flavour and fragrance additive in food, household cleaning products, cosmetics and perfumes [24]. Thus, it is also consumed by the human body through several ways. The hydrolytic half-life of *d*-limonene is >1000 days as described earlier [25]. Beside this limonene has been shown to prevent mammary, liver, lung, and other cancers. It has also been focused to treat a class of rodent cancers, including breast and pancreatic carcinomas. Being a good solvent of cholesterol, d-limonene has been exploited clinically to dissolve cholesterol-containing gallstones [26]. Owing to its gastric acid neutralizing effect and its support of normal peristalsis, it has also been utilized for relief of heartburn and gastroesophageal reflux (GERD).

Limonene is a constituent in a class of cosmetics, pharmaceuticals, solvents so this study has greater importance with human health concern. In the present work, we demonstrated the binding of limonene to BSA by employing Fluorescence, CD, UV-visible spectroscopic methods and effect of limonene on the conformation and stability of BSA was further checked by the help of DLS and DSC respectively. In addition to this molecular docking and displacement studies were also done to reveal binding site of

limonene. BSA and limonene both are antioxidants, and this property may be synergistically increased upon BSA-limonene complex formation. The present study may be helpful to postulate how herbivores combat free radical scavenging by exploring binding efficacy of limonene to BSA.

## *2. Materials and Methods*

### 2.1 *Materials*

Essentially fatty acid free bovine serum albumin (A7030) and (R)-(+)-Limonene (183164) were products of Sigma-Aldrich, INDIA. All other reagents were of analytical grade.

### 2.2 *Preparation of solutions*

All experiments were carried out in 20 mM phosphate buffer, pH 7.4. BSA was used without further purification as its purity was checked by SDS–PAGE at high concentration. BSA was dialyzed properly against respective buffer. Protein stock solutions (5mg/ml) were prepared in 20 mM phosphate buffer, pH 7.4. The concentration of native proteins in 20 mM phosphate buffer was determined spectrophotometrically from the extinction coefficient reported at 280 nm.

### 2.3 *UV-Visible Spectroscopic measurements*

Absorption measurements were performed at 37 °C Perkin-Elmer Lambda 25 double beam UV–Vis spectrophotometer attached with peltier temperature programmer-1 (PTP–1). A fixed concentration of BSA (6 μM) and limonene (6 μM) (molar ratio of P: L = 1:1) were taken and spectra was measured.

### 2.4 *Steady state fluorescence quenching measurements*

Schimadzu 5301 PC fluorescence spectrophotometer is equipped with a constant temperature holder and the temperatures (15, 25 and 37 °C) were maintained by a constant temperature water circulator (Julabo Eyela). The excitation and emission slits width were set at 3 nm. The titration of the limonene (0–30 μM) to 2 μM BSA solutions was carried out in a dual-path length fluorescence cuvette (10×3.5 mm). The shorter path length was oriented towards the emission side. Such a low concentration of BSA (2 μM) with absorbance value of ~0.07 was used throughout the fluorescence experiments to minimize the inner filter effect. Intrinsic fluorescence was measured by exciting at 280 nm. The emission spectra were recorded in the range of 300-450 nm and the data were plotted at 339 nm. The decrease in fluorescence intensity at 339 nm was analyzed according to the Stern–Volmer Equation 1:

$$F_o/F = K_{sv}[Q] + 1 = k_q \tau_o [Q] + 1 \quad (1)$$

where $F_o$ and F were the fluorescence intensities in absence and presence of quencher (limonene), $K_{sv}$ is the Stern–Volmer quenching constant, $k_q$ is the bimolecular rate constant of the quenching reaction and $\tau_0$ the average integral fluorescence life time of tryptophan which is $\sim 10^{-9}$ sec. Binding constants and binding sites were obtained from Equation 2:

$$\text{Log}\,(F_o/F - 1) = \log K_b + n \log [Q] \quad (2)$$

Where $K_b$ is the binding constant and n is the number of binding sites. The change in free energy was calculated from Equation 3 whereas change in enthalpy and entropy at different temperatures were analysed from the van't Hoff equation as given in Equation 4:

$$\Delta G^\circ = -RT ln K_b \quad (3)$$

$$lnK_b = \frac{-\Delta H^\circ}{RT} + \frac{\Delta S^\circ}{R} \quad (4)$$

Where ΔG° is free energy change, ΔH° is the enthalpy change, ΔS° is entropy change, R (1.987 cal $mol^{-1}K^{-1}$) is a gas constant and T is the absolute temperature (K).

The synchronous fluorescence spectra were recorded at Δλ 15(for tyrosine) and 60nm (for tryptophan) in the absence and presence of limonene over a wavelength range of 290–350 nm.

The three-dimensional fluorescence spectra were measured under the following conditions: the emission wavelength was recorded between 200 and 500 nm, the initial excitation wavelength was set at 200 nm with an increment of 5 nm, the number of scanning curves was 31, and the other scanning parameters were just the same as those of the fluorescence emission spectra.

2.5 *Fluorescence resonance energy transfer (FRET) to the limonene*

The fluorescence spectra of BSA (2 μM) and absorption spectra of limonene (2 μM) between 300 to 400 nm were scanned in similar way as given in method sections 'Fluorescence Quenching' and 'UV-Visible' experiments at 25 °C. If the emission spectrum of donor (BSA) significantly overlaps with the absorption spectrum of acceptor (limonene), these donor-acceptor pairs will considered in Förster distance and the possibility of energy transfer between them could be ascertained [27]. Therefore, the degree of energy transfer depends upon the area of overlap and the distance between these donor-acceptor molecules. The efficiency of energy transfer (E) is calculated using the following Equation 5:

$$E = 1 - \frac{F}{F_0} = \frac{R_0^6}{R_0^6 + r^6} \quad (5)$$

Where $F_o$ and F were the fluorescence intensities of BSA in absence and presence of limonene respectively; r is the distance between donor and acceptor and $R_o$ is the critical distance at which transfer efficiency equals to 50% which can be calculated from the following Equation:

$$R_0^6 = 8.79 \times 10^{-25} K^2 n^{-4} \emptyset J \quad (6)$$

where $K^2$ is the orientation factor related to the geometry of the donor and acceptor of dipoles, $n$ is the refractive index of the medium, φ is the fluorescence quantum yield of the donor in absence of acceptor; and $J$ expresses the degree of spectral overlap between the donor emission and the acceptor absorption which can be evaluated by integrating the overlap spectral area in between 300 to 400 nm from following Equation:

$$J = \int_0^\infty \frac{F(\lambda)\varepsilon\lambda^4 d\lambda}{\int_0^\infty F(\lambda) d\lambda} \quad (7)$$

Where F (λ) is the fluorescence intensity of the donor at wavelength range λ which is dimensionless, and ε (λ) is the molar absorptivity (extinction coefficient) of the acceptor wavelength λ in $M^{-1}cm^{-1}$. In our present study $K^2$, φ and $n$ were taken as 2/3, 0.118 and 1.336 respectively[28].

2.6 *Circular dichroic measurements*

The isothermal wavelength scan studies of BSA in the absence and presence of limonene were carried out with JASCO-J815 spectro polarimeter equipped with a Peltier-type temperature controller. The instrument was calibrated with d-10-camphorsulfonic acid. All the isothermal CD measurements were made at 25°C. Spectra were collected with 50 nm/min scan speed, 0.1 nm data pitch and a response time of 2 s. Each spectrum was the average of 2 scans. For far-UV CD spectra (190-250 nm) and near-UV CD (250-300 nm) the cells of 0.1 cm and 1 cm path length were taken. Helical content was

calculated by using online available $K_2D$ software. All spectra were smoothed by the Savitzky–Golay method with 25 convolution width. BSA concentrations used for far-UV CD and near-UV CD were 2 μM and 15 μM respectively

2.7 *Differential scanning calorimetry*

The differential scanning calorimetric measurements were carried out using VP-DSC micro calorimeter (Micro Cal, Northampton, MA). The buffer and protein solutions were degassed under mild vacuum prior to the experiment. Samples were prepared in 20 mM sodium phosphate buffer, pH 7.4. The DSC measurements of BSA (18 μM) in the presence of 1:15 ratio of limonene were performed from 25 to 90°C at a scan rate of 0.5°C/min. Data was analyzed using Origin software provided with the instrument to obtain the temperature at the midpoint of the unfolding transition (Tm) and calorimetric enthalpy (ΔH°).

2.8 *Dynamic light scattering (DLS) measurements*

DLS measurements were carried out at 830 nm by using DynaPro-TC-04 dynamic light scattering equipment (Protein Solutions, Wyatt Technology, Santa Barbara, CA) equipped with a temperature-controlled micro sampler. BSA (2 mg/ml) was incubated with the limonene for 8 hours. The samples were spun at 10,000 rpm for 10 min and were filtered serially through 0.22 and 0.02 μm Whatman syringe filters directly into a 12 μl quartz cuvette. For each experiment, 20 measurements were taken. Mean hydrodynamic radius ($R_h$) and polydispersity were analysed using Dynamics 6.10.0.10 software at optimized resolution. The $R_h$ was estimated on the basis of an autocorrelation analysis of scattered light intensity data based on translation diffusion coefficient by Stoke's-Einstein relationship:

$$R_h = \frac{kT}{6\pi\eta D} \quad (8)$$

where $R_h$ is the hydrodynamic radius, $k$ is Boltzmann constant, $T$ is the temperature, $\eta$ is the viscosity of water and $D$ is diffusion coefficient [29].

2.9 *Molecular docking and Binding Displacement Measurement study Using Site Markers*

To determine the amino acid residue involved in binding site of limonene on BSA the docking studies were performed by auto dock 4.2.0 software (http://autodock.scripps.edu) as reported earlier [30]. Lamarckian genetic algorithm (LGA) implemented with an adaptive local method search was applied to determine the possible conformation of the drug that binds to the protein [31]. The crystal structure of BSA was obtained from Brookhaven Protein Data Bank having PDB id (4F5S) and 3d sdf file of limonene (CID 22311) was obtained from PubChem. Water molecules and hydrogen atoms were removed from the protein. Then partial Kollman charges were assigned to BSA. Protein was held rigid and all torsional bonds are taken as being free during docking calculations.

Moreover, the protein was set to be rigid and there is no consideration of solvent molecules on docking. To determine the binding site on BSA blind docking was carried out and the grid size was set to be 126, 126 and 126 along X, Y and Z axes with 0.564 Angstrom grid spacing. Auto dock parameters were used with GA population size:150 and maximum number of energy evolutions:250,0000. 10 best solution based on docking score was retained for further analysis, Discovery studio 3.5 were used for visualization and for the identification of residues involved in binding. Binding displacement studies between limonene and BSA in the presence of two site markers, warfarin (for site I) and

diazepam (for site II) were measured using the fluorescence titration method. The titration of limonene was carried out to the solution having protein and site marker in the ratio of 1:1 and the Ksv values were calculated by using Equation 1.

## 3. Results and Discussion

### 3.1 *UV-visible absorption spectroscopy*

Ultraviolet-visible absorption spectroscopy is an influential tool for steady-state studies of protein-drug interaction. Changes in far and near UV regions correspond to secondary and tertiary structure respectively. In proteins, we discriminate various internal chromophoric groups that give rise to electronic absorption bands. The aromatic amino acids contribute to bands in the range of 255-300 nm. In Fig. 1A shows that the absorption peak of BSA centres at ~280 nm mainly due to tryptophan residue. However, after addition of the limonene, the maximal absorption peak as well as absorption intensity of BSA is increased. This indicated that the interaction of limonene leads to the conformational change in BSA which is primarily near to the tryptophan residue. In Fig. 1A, the maximum change was observed at 280 nm where the increase in absorbance with 6μM limonene indicates complex formation between BSA and limonene.

### 3.2 *Tryptophan fluorescence quenching by limonene*

Tryptophan fluorescence quenching was performed for the determination of interaction between limonene and BSA by titration of limonene against protein at 25°C. BSA has a strong fluorescence emission peak at ~339 nm on excitation at 280 nm, addition of the limonene caused reduction in the emission spectra of BSA as shown in Fig. 1B. The values of emission intensity at 339 nm were used to measure drug–binding affinity. The fluorescence intensity of tryptophan fluorescence emission decreases

continuously but at higher concentration of limonene the decreasing pattern of emission gets saturated which is a clear indication of binding of limonene to a specific binding site on BSA. The same experimental procedures were also followed at 15 and 37 $^{\circ}$C where we found that on increasing the temperature, the quenching also decreases, or in other words, the extent of lowering in fluorescence emission was higher at lower temperature. The decrease in fluorescence intensity upon addition of limonene was analysed according to the Stern-Volmer equation (as shown in Fig. 2A). There is a linear dependence between $F_o/F$ and molar concentration of the limonene in Stern-Volmer plot. The slopes decrease with increasing temperature, means the ligand binding to the protein was occurred by 'static quenching'. When the value of kq was calculated it was greater than maximum scatter collision quenching constant i.e. $2.0 \times 10^{10}$ $mol^{-1}s^{-1}$[32]. This shows that quenching is not initiated by dynamic diffusion but occurs by formation of a strong complex between BSA and limonene. Moreover, the absorption spectra of BSA-limonene (Fig. 1A) were transparently different from those of BSA or limonene alone that give clear proof of forming a protein drug complex with a new structure. From the obtained results, it is to be noted that static type of quenching occurs during the binding of limonene with BSA. The Ksv values for limonene at different temperature are given in the Table 1.

3.3 *Determination of binding constant and number of binding sites*

For the determination of the binding constant and number of binding sites log [($F_0$ /F) -1] v/s log [limonene] was plotted (Fig. 2B). By using equation 2 from the slopes and intercepts of modified Stern-Volmer plots number of binding sites (n) and the value of binding constant were calculated respectively. For limonene, the values of $K_b$ and *n* were

calculated at different temperatures and the observed values are listed in Table 1. The data shows that decrease in $K_{sv}$ or decrease in $K_b$ on increasing the temperature is a clear indication of static quenching[33].

*3.4 Thermodynamics of BSA-limonene interaction*

Generally, a small molecule binds to a macromolecule by the following four binding modes: hydrogen bonds, van der Waals attractions, electrostatic interactions, and hydrophobic interactions. The thermodynamic parameters, enthalpy change (ΔH) and entropy change (ΔS) of the reaction, are very important for confirming binding modes. The temperature-dependence of the binding constant was investigated at three different temperatures (15, 25 and 37°C), by considering that BSA could not undergo any structural degradation

According to the binding constants of limonene to BSA at the three different temperatures, the thermodynamic parameters were determined from linear second law of thermodynamics plot (Fig. 3) and the observed values are presented in Table 1. For the determination of enthalpy-entropy relation in BSA-limonene interaction, three temperatures *viz*. 15, 25 and 37 $^{o}$C are considered only because during the binding process the structure of the protein assume to be structurally unaltered as major conformational changes gives the false reading of thermodynamic parameters for interaction studies. In other words, the obtained enthalpy-entropy changes are mainly caused by the binding of the limonene molecules to BSA. As shown in Table 1, ΔG in every condition is negative which suggested that interaction process is spontaneous, ΔH and ΔS for the complex formation between limonene and BSA are found to be -7.2 kcal.mol$^{-1}$ and -6.53 cal.mol$^{-1}$K$^{-1}$ respectively. Thus, the interaction of limonene with

BSA is an exothermic reaction accompanied by negative ΔS value. Negative ΔS value suggested that the bound water to the protein molecule in or near the binding pockets did not disturb and BSA is stabilized in the presence of limonene as further confirmed by CD and DSC.

*3.5 Energy transfer between BSA and limonene*

A possibility of energy transfer between BSA and limonene was investigated for further confirmation of the proximity of binding. Fig. 4 shows the spectral overlap between the emission spectrum of BSA and the UV–absorption spectra of the limonene with the molar ratio of BSA: limonene (donor: acceptor) as 1. $R_o$ and r were calculated by using J value $7.74 \times 10^{-16}$ $cm^3M^{-1}$ and values obtained for BSA-limonene complex are 1.6 and 2.3 nm respectively. The energy transfer took place from BSA to limonene with great possibility. The distance between donor and acceptor was on the scale of 2–8 nm that satisfies $0.5R_o < r < 1.5R_o$ in accordance with Förster's non–radiative energy transfer theory [34, 35]. The range of r values do not exceed the dimensions of the protein (8×8×3 nm) which shows that the energy–transfer from BSA to limonene is possible. This further justifies that the energy transfer between BSA and limonene contributes to the noticeable decrease of protein fluorescence intensity through static quenching mechanism[36]. FRET results are listed in Table 4.

*3.6 Synchronous fluorescence spectroscopy studies*

Synchronous fluorescence spectroscopy was used to measure the fluorescence quenching and also provide information about the conformational changes in the protein. The possible shift of the maximum emission wavelength $\lambda_{max}$ is related to the alteration of the polarity around the chromophore micro-environment [35], representing the value of

difference between excitation and emission wavelength. When the values of Δλ are stabilized at 15 or 60 nm, the synchronous fluorescence gives the characteristic information of tyrosine and tryptophan residues, respectively [37]. The synchronous fluorescence spectra of BSA–limonene system are shown in Fig. 5. The maximum emission wavelength has negligible shift when Δλ fixed at 15 nm. This expressed that the conformation of BSA was unchanged around tyrosine residue [35]. Although in Fig. 5B, the maximum emission wavelength has red shift in the presence of limonene when Δλ fixed at 60 nm. This implied that limonene has more chance to cause conformational changes close to tryptophan residues than tyrosine [37]. Moreover, the fluorescence intensity decreased regularly with the addition of limonene in both systems (Fig. 5A&5B), which further depicted the occurrence of fluorescence quenching in the binding process.

*3.7 Three dimensional fluorescence spectroscopic analysis*

To study the conformational changes in BSA upon addition of limonene (Fig. 6) three dimensional fluorescence spectra was measured and related parameter are shown in Table 2. Peak 1 is the Rayleigh scattering peak (λex = λem**)**, peak 4 **is** second order scattering peak (λex = 2λem). Peak 2 and peak 3 are the two typical fluorescence peaks. It is shown in figure that both peak 2 (333.5→313.2 nm) and peak 3 (261→252.9 nm) of BSA were quenched by limonene with no shift of emission wavelength whereas Rayleigh scattering peaks were enhanced that gives clear evidence of complex formation[32]. Peak 2 mainly reflects the spectral behaviour of Trp which is mainly caused by the transition of $n \rightarrow \Pi^*$ of aromatic amino acids in BSA. Peak 3 exhibits the spectral characteristics of polypeptide backbone ( $\Pi \rightarrow \Pi^*$ transition ) [38]. All these results and analysis deciphered

that the binding of limonene to BSA induced conformational and micro environmental changes.

*3.8 Circular Dichroism measurement*

Circular Dichroism (CD) is an imperative technique in biological chemistry and structural biology especially for secondary structure determination [39]. Spectra in the far-ultraviolet wavelength range (typically from ~200 to 250 nm) provide information on the polypeptide backbone conformations of proteins. Secondary structural elements, such as α-helices, β- sheets, β turns, and random coil structures, all make bands of individual shapes and magnitudes in the far ultraviolet region. Due to the binding of ligands to globular protein, the intermolecular forces liable for sustaining the secondary and tertiary structures can be rehabilitated triggering in a conformational alteration of the protein.

In order to obtain an insight in to the structure of BSA, the far-UV CD spectra were recorded in presence and absence of limonene and are shown in Fig. 7. The CD spectrum of BSA exhibited two negative minima in UV region at 208 and 222 nm which is characteristic of α-helix structure of the protein. The similar spectral features were noticed in our previous report [40]. The binding of limonene to BSA increased both (208 and 222 nm) of these negative minima peaks, clearly indicating the induction of α-helix structure of protein upon interaction with the limonene. Further, the CD spectra of BSA in the presence of limonene were found to be similar in shape, revealing that the structure of BSA is predominantly α-helix even after the addition of limonene. Using $K_2D$ software, the α-helicity of BSA was calculated. It increased from 62% to 66.80% in the presence of 30 μM limonene. Overall it is clearer from spectra that BSA is more stabilized in the presence of 30 μM of limonene rather than 10 μM. Near UV CD spectra

(250-320 nm) exhibited changes around 263 nm on addition of limonene to BSA [Fig 7 B]. This signposted that both the secondary as well as tertiary structures of BSA are changed due to limonene binding.

*3.9 Thermo stability study of limonene–BSA interaction by Differential scanning calorimetry*

Generally, ligand binding either stabilize or destabilize the proteins. DSC was employed to investigate the effect of limonene on the thermal stability of BSA. $\Delta T_m$ and $\Delta H$ are the two main parameters obtained from DSC are giving the information about the effect of ligand binding on the thermal stability of protein. Fig. 9 shows the DSC thermo grams for BSA: limonene in the molar ratio of 1:0, 1:15. BSA unfolds cooperatively and gives a single endothermic peak with melting temperatures of (61.14 $^0$C) [41]. It is observed that thermal denaturation of BSA was found to be only partially reversible under the conditions of this study. Under saturating conditions limonene stabilized the BSA as evidenced by escalation in melting temperature $\Delta T_m$ by 3.0 $^0$C also accompanied by increase in enthalpy value. These results indicated that the binding stabilizes the protein structure linearly with the CD results.

*3.10 Dynamic light scattering Study*

It was clear from the above investigations that upon interaction with limonene, BSA undergoes conformational changes. Conformational changes might be affected the size of protein molecules. Dynamic light scattering was used to examine the hydrodynamic radius of native BSA and BSA− limonene complex. In Fig. 8, the hydrodynamic radii of native BSA and BSA in the presence of limonene were plotted and observed data shown in Table 3. Polydispersity is the parameter to tell about

homogeneity of solution [42]. The value of hydrodynamic radius (3.7 nm) for native BSA is satisfactory with earlier reports[43]. The hydrodynamic radii of BSA complexes with limonene got fall down than the BSA alone. The reduction in hydrodynamic radii upon ligand binding may be due to the "collapsing" of protein as limonene binds with BSA. This response may outcome shrinkage in the molecular volume due to a conformational alteration similar results were reported for HSA in the presence of pollutants [44]. The possible mechanism for drop in protein hydrodynamic radius is that limonene disrupts the solvent shell around the BSA.

Two molar ratios of BSA and limonene, 1:5 and 1:15 were taken to observe the effect of limonene on protein dynamics and results indicated continuous shrinkage in hydrodynamic radius. As CD data suggested limonene affects the secondary and tertiary structure of BSA. This also might be a reason that secondary structural components conformational altered tends to decrease in hydrodynamic radius.

*3.11 Molecular docking study and Binding Displacement Measurement Using Site Markers*

The molecular docking study was performed to further reveal the interaction of limonene with BSA. The BSA comprises of three homologous domains, each domain made up of subdomains that possess common structural motifs. The principal regions of ligand binding to BSA are located in hydrophobic cavities in subdomains IIA and IIIA, which are consistent with Sudlow sites I and II, respectively [12]. In the present study, Auto dock 4.2.0 program was applied to calculate the possible conformation of the limonene that binds to the BSA. The best energy ranked results are summarized in Table 5. Fig10 A & 10 B show that limonene more favorably fit in the hydrophobic pocket close to

Sudlow site I in domain IIA with ΔG and $K_b$ of -4.64 kcal $mol^{-1}$, $2.4\times10^3$ $M^{-1}$ respectively. By using the equation 3, the binding constants (Kb) for protein-ligand interactions were calculated from the obtained free energy changes of docking. The Tyr149, Arg217, Leu237, Arg256, Leu259, Ala260, Ile263, Ser286, Ile289, and Ala290 of site I are involved in hydrophobic interaction[45] [46]. Interaction parameters including $K_b$ and $\Delta G$ are agreed well with the results from the fluorescence quenching measurements. Therefore, molecular docking in this study yields useful information about the specific residues of BSA involved in the interactions with the limonene for better understanding of protein-ligand interaction at the molecular level. For further confirmation of site involved in the binding of limonene with BSA, displacement study was done by exploiting standard site markers, warfarin for site I[47] and diazepam for site II. The Ksv value of BSA-limonene was ($1.14\times10^4$) that decreases to ($1.0\times10^4$) and ($2.03\times10^3$) in presence of diazepam and warfarin, respectively. These differences in Ksv values in absence and presence of site markers are significant enough to deduce the binding sites location as reported in literature [48, 49]. As evident from above values, the Ksv of BSA-limonene decreased markedly in presence of warfarin. It indicates limonene binds to close to Sudlow site I in domain IIA of BSA as Ksv was remain same in case of diazepam and decreased with warfarin.

## Conclusions

In the present work, we have computed the binding parameters, conformational alterations leading to enhance in stability of BSA-limonene complex by using different spectroscopic, calorimetric and molecular docking methods. Putting all results together, it is to be concluded that limonene binds with BSA via static quenching manner and the

binding process is spontaneous and exothermic. DSC and CD results enlighten the limonene as a stabilizer of BSA, molecular docking and displacement study reveals the binding site of limonene close to Sudlow site I in domain IIA of BSA. BSA as a drug carrier may aid in the delivery of limonene to an inflamed region and facilitate drug access.

**Acknowledgements**

Facilities provided by I.B.U, Aligarh Muslim University are gratefully acknowledged. S.K.C, EA, J.M.K and P.A are highly thankful to the Council of Scientific and Industrial Research, New Delhi, for financial assistance in the form of senior research fellowship (SRF) and junior research fellowship (JRF).

**References:**

1. B. Eyheraguibel, C. Richard, G. Ledoigt and A. Ter Halle, *J Agric Food Chem*, 2011, **59**, 4868-4873.
2. T. Kaur, K. Hussain, S. Koul, R. Vishwakarma and D. Vyas, *PLoS One*, 2013, **8**, e69112.
3. G. Zolese, G. Falcioni, E. Bertoli, R. Galeazzi, M. Wozniak, Z. Wypych, E. Gratton and A. Ambrosini, *Proteins*, 2000, **40**, 39-48.
4. H. Xu, Q. Liu and Y. Zuo, *J Solution Chem*, 2009, **38**, 15-25.
5. P. M. Hua-Xin Zhang, *J Solution Chem*, 2009, **38**, 351-361.
6. Y. Q. Wang, H. M. Zhang, G. C. Zhang, W. H. Tao, Z. H. Fei and Z. T. Liu, *J Pharm Biomed Anal*, 2007, **43**, 1869-1875.
7. Y.-Z. L. Neng Zhou, Ping Wang, *Journal of Photochemistry and Photobiology A: Chemistry*, 2007, **185**, 271-276.
8. C. Bertucci, S. Cimitan, A. Riva and P. Morazzoni, *J Pharm Biomed Anal*, 2006, **42**, 81-87.
9. Y. L. Yan-Jun Hu, Ru-Ming Zhao, Jia-Xin Dong, Song-Sheng Qu, *Journal of Photochemistry and Photobiology A: Chemistry*, 2006, **179**, 324-329.
10. Y.-l. W. Ya-Ping Wang, Chuan Dong, *Journal of Photochemistry and Photobiology A: Chemistry*, 2006, **177**, 6-11.
11. U. Kragh-Hansen, *Pharmacol Rev*, 1981, **33**, 17-53.

12. D. C. Carter, B. Chang, J. X. Ho, K. Keeling and Z. Krishnasami, *Eur J Biochem*, 1994, **226**, 1049-1052.
13. J. R. Lakowicz, *Springer, New York*, 2008, **3rd edn**.
14. Y. J. Hu, W. Li, Y. Liu, J. X. Dong and S. S. Qu, *J Pharm Biomed Anal*, 2005, **39**, 740-745.
15. C. Dufour and O. Dangles, *Biochim Biophys Acta*, 2005, **1721**, 164-173.
16. S. Bi, D. Song, Y. Tian, X. Zhou, Z. Liu and H. Zhang, *Spectrochim Acta A Mol Biomol Spectrosc*, 2005, **61**, 629-636.
17. Y. Q. Wang, H. M. Zhang and G. C. Zhang, *J Pharm Biomed Anal*, 2006, **41**, 1041-1046.
18. X. F. Liu, Y. M. Xia and Y. Fang, *J Inorg Biochem*, 2005, **99**, 1449-1457.
19. M. I. Kaldas, U. K. Walle, H. van der Woude, J. M. McMillan and T. Walle, *J Agric Food Chem*, 2005, **53**, 4194-4197.
20. X. Long, S. Liu, L. Kong, Z. Liu and S. Bi, *Talanta*, 2004, **63**, 279-286.
21. A. Papadopoulou, R. J. Green and R. A. Frazier, *J Agric Food Chem*, 2005, **53**, 158-163.
22. J. Namiesnik, K. Vearasilp, A. Nemirovski, H. Leontowicz, M. Leontowicz, P. Pasko, A. L. Martinez-Ayala, G. A. Gonzalez-Aguilar, M. Suhaj and S. Gorinstein, *Appl Biochem Biotechnol*, 2014, **172**, 2849-2865.
23. F. Sheng, Y. Wang, X. Zhao, N. Tian, H. Hu and P. Li, *J Agric Food Chem*, 2014, **62**, 6813-6819.
24. Y. W. Kim, M. J. Kim, B. Y. Chung, Y. Bang du, S. K. Lim, S. M. Choi, D. S. Lim, M. C. Cho, K. Yoon, H. S. Kim, K. B. Kim, Y. S. Kim, S. J. Kwack and B. M. Lee, *J Toxicol Environ Health B Crit Rev*, 2013, **16**, 17-38.
25. W. F. Hink and B. J. Fee, *J Med Entomol*, 1986, **23**, 400-404.
26. H. Igimi, T. Hisatsugu and M. Nishimura, *Am J Dig Dis*, 1976, **21**, 926-939.
27. T. Förster, *Ann. Phys. 2*, 1948, **473**, 55-75.
28. Q. Wang, X. Liu, M. Su, Z. Shi and H. Sun, *New Journal of Chemistry*, 2014.
29. E. Ahmad, P. Sen and R. H. Khan, *Cell Biochem Biophys*, 2011, **61**, 313-325.
30. N. Jiang, C. Yang, X. Dong, X. Sun, D. Zhang and C. Liu, *Org Biomol Chem*, 2014, **12**, 5250-5259.
31. G. M. Morris, R. Huey, W. Lindstrom, M. F. Sanner, R. K. Belew, D. S. Goodsell and A. J. Olson, *J Comput Chem*, 2009, **30**, 2785-2791.
32. M. Ishtikhar, S. Khan, G. Badr, A. Osama Mohamed and R. Hasan Khan, *Molecular BioSystems*, **10**, 2954-2964.
33. S. R. Feroz, S. B. Mohamad, N. Bujang, S. N. A. Malek and S. Tayyab, *Journal of Agricultural and Food Chemistry*, 2012, **60**, 5899-5908.
34. Y.-J. Hu, Y. Liu, L.-X. Zhang, R.-M. Zhao and S.-S. Qu, *Journal of Molecular Structure*, 2005, **750**, 174-178.
35. A. Varlan and M. Hillebrand, *Molecules*, 2010, **15**, 3905-3919.
36. Z. Chi, R. Liu, Y. Teng, X. Fang and C. Gao, *Journal of Agricultural and Food Chemistry*, 2010, **58**, 10262-10269.
37. A. Bhogale, N. Patel, J. Mariam, P. M. Dongre, A. Miotello and D. C. Kothari, *Colloids Surf B Biointerfaces*, 2014, **113**, 276-284.
38. S. Sugio, A. Kashima, S. Mochizuki, M. Noda and K. Kobayashi, *Protein Eng*, 1999, **12**, 439-446.
39. P. Kumar, B. Baidya, S. K. Chaturvedi, R. H. Khan, D. Manna and B. Mondal, *Inorganica Chimica Acta*, 2011, **376**, 264-270.
40. J. M. Khan, S. A. Abdulrehman, F. K. Zaidi, S. Gourinath and R. H. Khan, *Phys Chem Chem Phys*, 2014, **16**, 5150-5161.
41. A. Y. Khan, M. Hossain and G. S. Kumar, *Mol Biol Rep*, 2013, **40**, 553-566.

42. M. Yu, Z. Ding, F. Jiang, X. Ding, J. Sun, S. Chen and G. Lv, *Spectrochim Acta A Mol Biomol Spectrosc*, 2011, **83**, 453-460.
43. J. M. Khan, S. K. Chaturvedi and R. H. Khan, *Biochemical and biophysical research communications*, 2014, **441**, 681-688.
44. E. Ahmad, G. Rabbani, N. Zaidi, B. Ahmad and R. H. Khan, *PLoS One*, 2012, **7**, e38372.
45. B. Yang, F. Hao, J. Li, K. Wei, W. Wang and R. Liu, *Food and Chemical Toxicology*, 2014, **65**, 227-232.
46. X. Tan and Z. Song, *RSC Advances*, 2014, **4**, 3263-3271.
47. J. Tian, J. Liu, Z. Hu and X. Chen, *Bioorganic & Medicinal Chemistry*, 2005, **13**, 4124-4129.
48. N. Zaidi, E. Ahmad, M. Rehan, G. Rabbani, M. R. Ajmal, Y. Zaidi, N. Subbarao and R. H. Khan, *J Phys Chem B*, 2013, **117**, 2595-2604.
49. Y. Song, Y. Liu, W. Liu, F. A. Villamena and J. L. Zweier, *RSC Advances*, 2014, **4**, 47649-47656.

## Legends to Figures

**Figure 1(A). Absorption spectra of BSA gradually titrated with limonene at 25 °C.** (A) Limonene only, (B) BSA = 6 μM and (C) BSA/limonene = 1

**Figure 1(B). Fluorescence quenching of BSA by limonene at 25°C.** [BSA = 2 μM; limonene = 0-30 μM]. The inset corresponds to molecular structure of Limonene.

**Figure 2(A). The Stern–Volmer plots for the binding of Limonene with BSA at 288** (▲), 298 (■) and 310 (♦) K. Excitation wavelength was 280 nm, [BSA = 2μM; limonene = 0-30 μM].

**Figure 2(B). Plot between log [($F_o$/F)-1] and log [limonene] for BSA–limonene interaction** at 288(▲), 298(■) and 310(♦) K. [BSA = 2 μM; limonene = 0-30 μM].

**Figure 3. van't Hoff plot for temperature dependence of $K_b$**. Obtained from BSA fluorescence quenching by limonene at 15, 25 and 37 °C.

**Figure 4. Fluorescence resonance energy transfer**. Spectral overlap of the fluorescence emission of BSA and absorption spectra of limonene [BSA = limonene = 2 μM].

**Figure 5**. **Synchronous fluorescence spectrum of BSA**: (A) Δλ = 15 nm; (B) Δλ = 60 nm; [BSA = 2 μM; limonene = 0-30 μM].

**Figure 6. Three-dimensional fluorescence spectra of BSA and the BSA-limonene system** (A) BSA = 2 μM, limonene = 0; (B) BSA = 2 μM, limonene = 2 μM.

**Figure 7** (A). **Secondary structural rearrangements**. The far-UV CD spectra of [2 μM BSA only, 2 μM BSA + 10 μM limonene and 2 μM BSA + 30 μM limonene].

**Figure 7 (B).** Near-UV CD spectra of BSA (15 μM) with increasing concentration of limonene (0-225 μM)

**Figure 8.** Hydrodynamic radii pattern of BSA in the absence and presence of limonene.

**Figure 9.** DSC thermo grams of BSA and its complex with limonene (BSA: limonene = 1:15).

**Figure 10.** MolecularDocking results of BSA complexed with limonene (A) limonene is shown in a stick representation, and BSA represented with ribbon model (B) Detailed view of the docking poses of BSA-limonene complex.

**Table 1.** Binding parameters of limonene interaction to BSA in 20 mM Phosphate buffer pH 7.4 at different temperature obtained and calculated from fluorescence quenching results.

| T (K) | $K_{sv}$ ($\times 10^4\ M^{-1}$) | $k_q$ ($\times 10^{13}\ M^{-1}\ S^{-1}$) | *n* | $K_b$ ($\times 10^4\ M^{-1}$) | ΔG (kcal.mol$^{-1}$) | ΔH (kcal.mol$^{-1}$) | ΔS (cal. mol$^{-1}$.K$^{-1}$) |
|---|---|---|---|---|---|---|---|
| 288 | 1.146 | 1.146 | 1.00 | 1.171 | -5.34 | | |
| 298 | 0.798 | 0.798 | 0.99 | 0.765 | -5.27 | -7.2 | -6.53 |
| 310 | 0.541 | 0.541 | 0.98 | 0.473 | -5.19 | | |

**Table 2.** Three dimensional fluorescence spectra characteristics parameters of the BSA and Limonene-BSA system

| System | Peak 2 (λex/ λem) (nm/nm) | Δλ (nm) | Peak 2 ( Intensity) | Peak 3 (λex/ λem) (nm/nm) | Δλ (nm) | Peak 3 (Intensity) |
|---|---|---|---|---|---|---|
| A.BSA | 280/340 | 60 | 333.5 | 225/345 | 120 | 261 |
| B.BSA: Limonene (1:1) | 280/340 | 60 | 313.2 | 225/345 | 120 | 252.9 |

**Table 3.** Hydrodynamic radii and polydispersity of BSA in absence and presence of limonene.

| Conditions | $R_h$ (nm) | Pd (%) |
|---|---|---|
| A. BSA | 3.7±0.04 | 17.0 |
| B. BSA+ Limonene (1:5) | 3.5±0.03,19.3± 0.35 | 11.7 |
| C. BSA+ Limonene (1:15) | 3.4±0.03, 10.9±0.2 | 11.0 |

**Table 4** FRET parameters obtained from BSA-limonene binding.

| $J$ ($cm^3M^{-1}$) | $R_0$ (nm) | r (nm) | $E_{FRET}$ |
|---|---|---|---|
| $7.74 \times 10^{-16}$ | 1.6 | 2.3 | 0.1 |

**Table 5** Molecular docking parameters obtained from BSA-limonene binding.

| Binding site | Amino acid residues | Forces involved | ΔG (k cal $mol^{-1}$) | $K_b$ ($M^{-1}$) |
|---|---|---|---|---|
| Site I | Tyr 149, Arg 217<br>Leu237, Arg 256<br>Leu 259, Ala 260<br>Ile 263, Ser 286<br>Ile 289, Ala 290 | Hydrophobic | -4.6 | $2.4\times10^{3}$ |

**Figure 1**

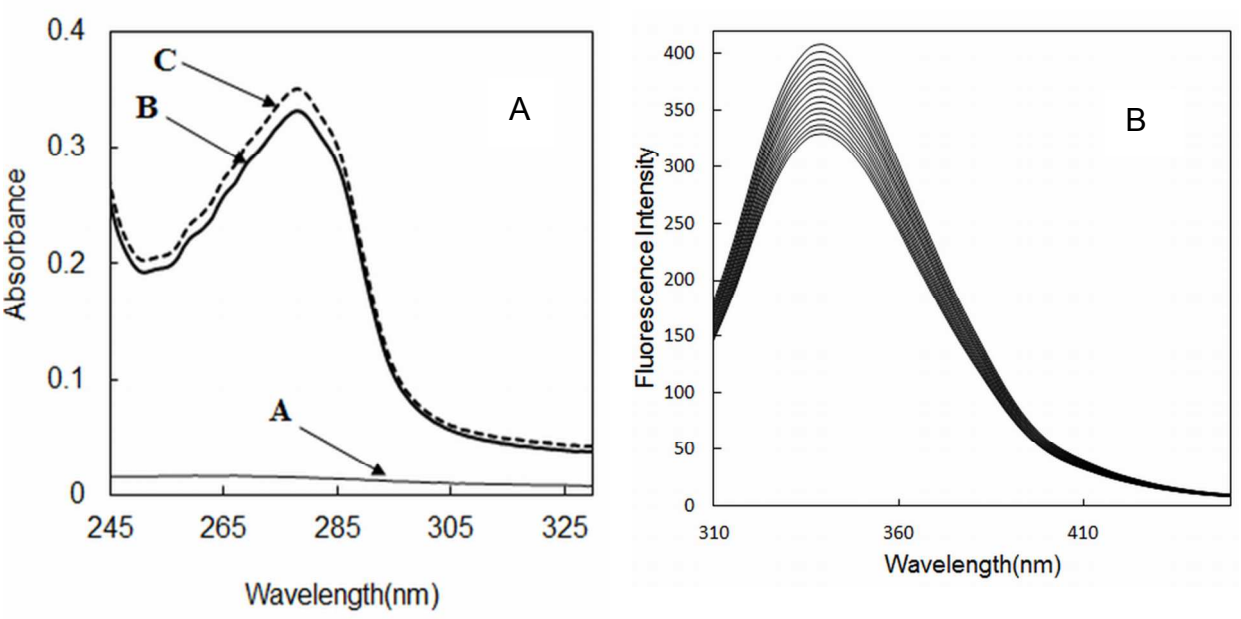

**Figure 2**

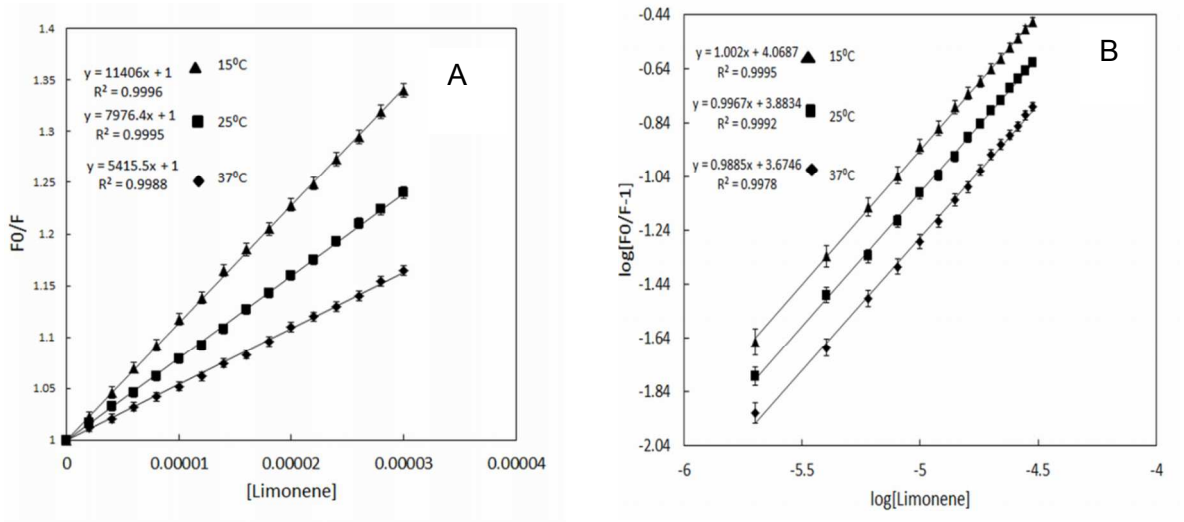

**Figure 3**

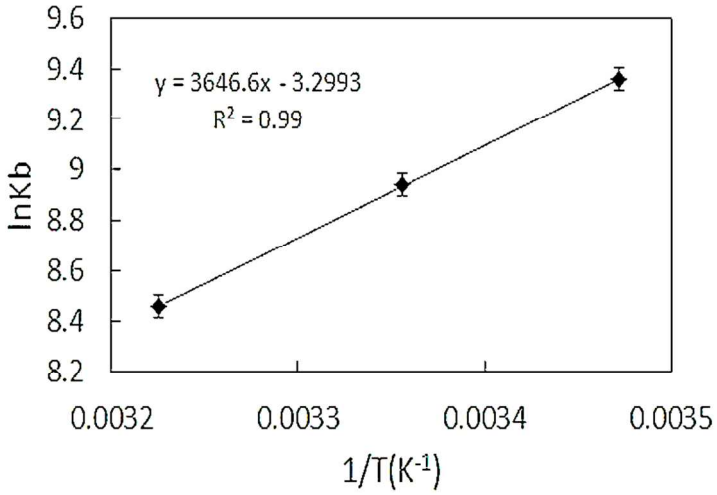

**Figure 4**

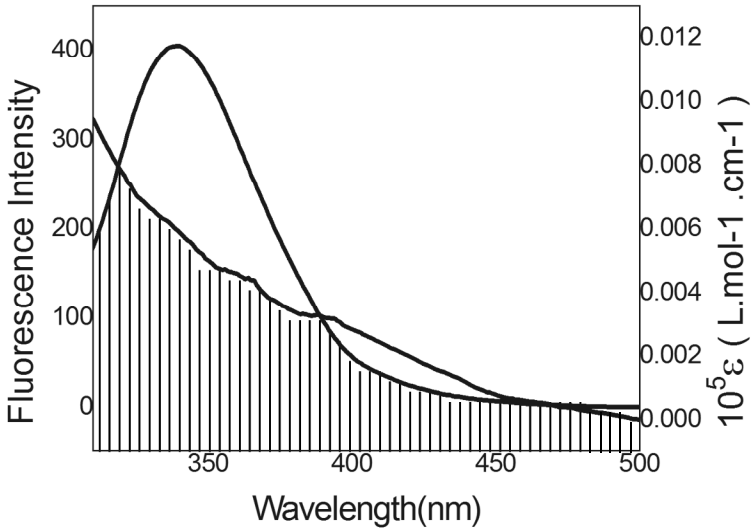

**Figure 5**

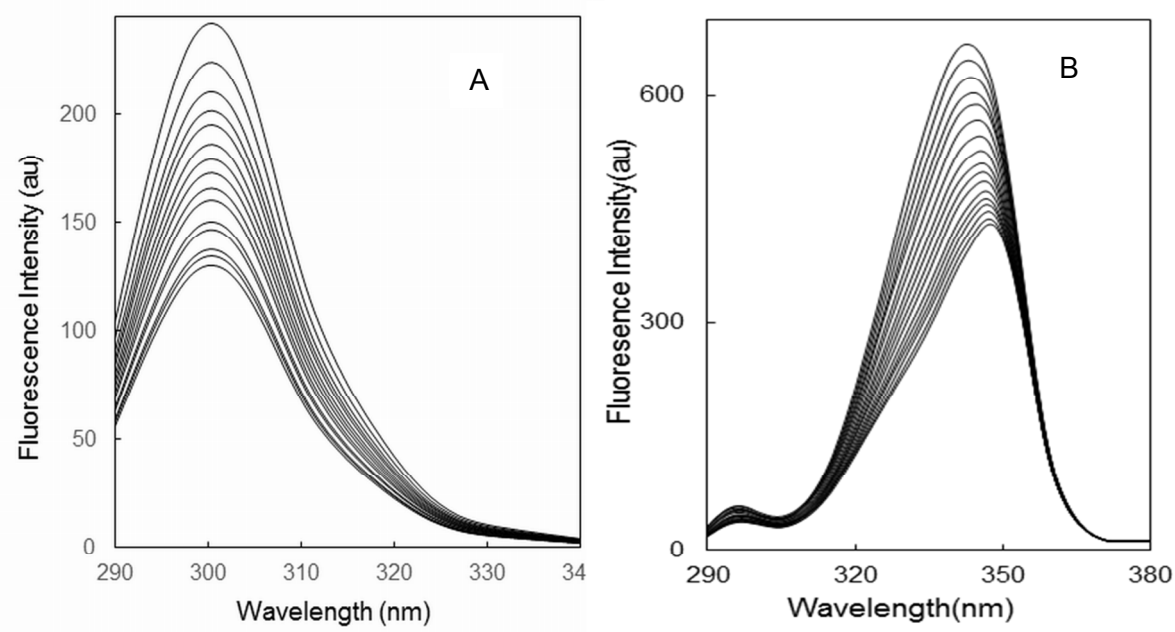

**Figure 6**

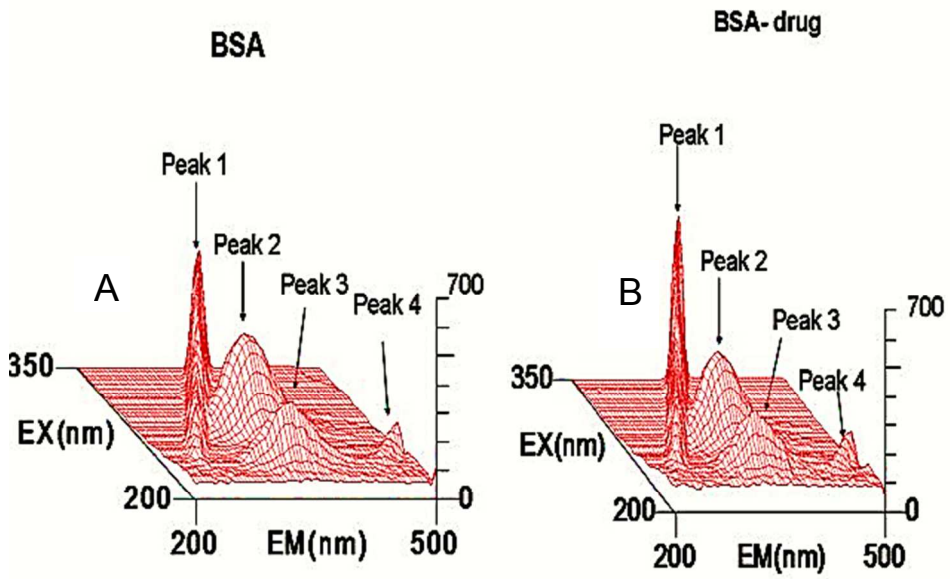

**Figure 7**

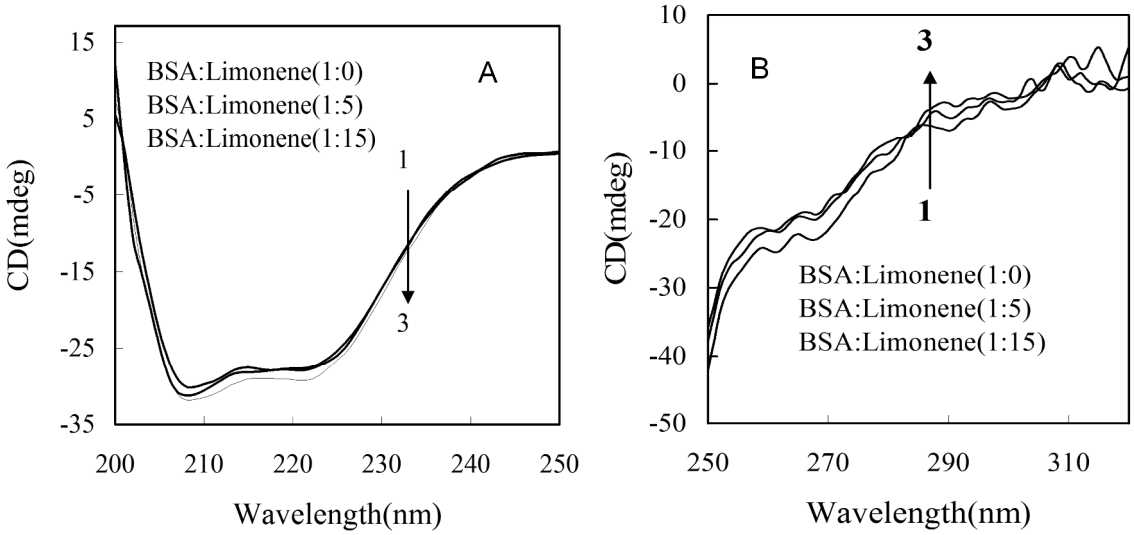

**Figure 8**

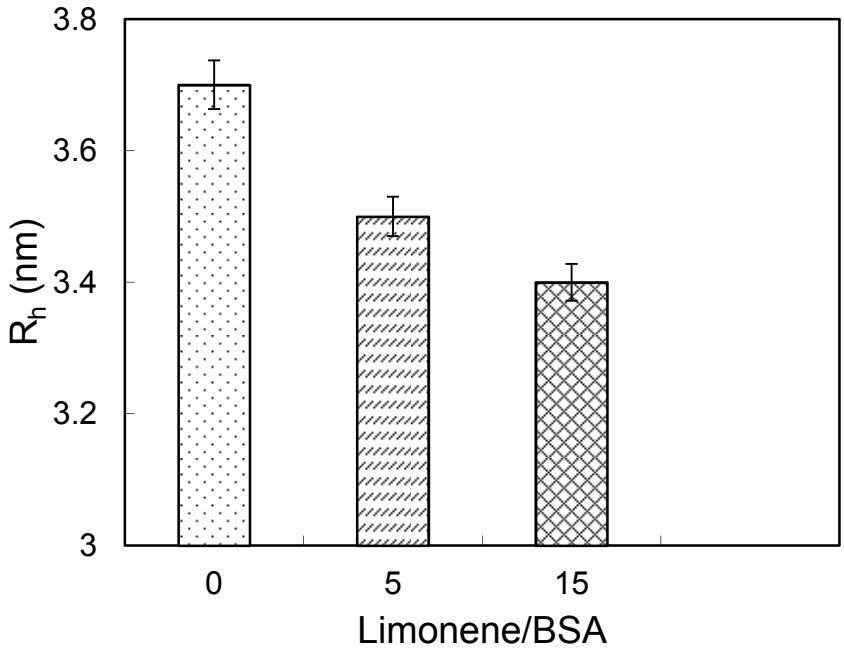

**Figure 9**

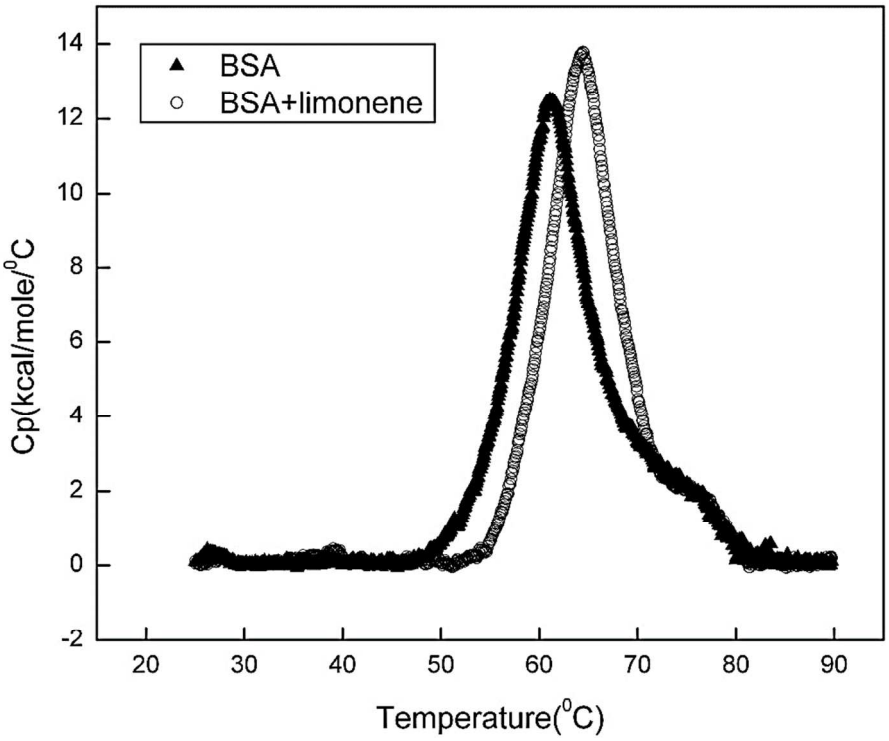

**Figure 10**

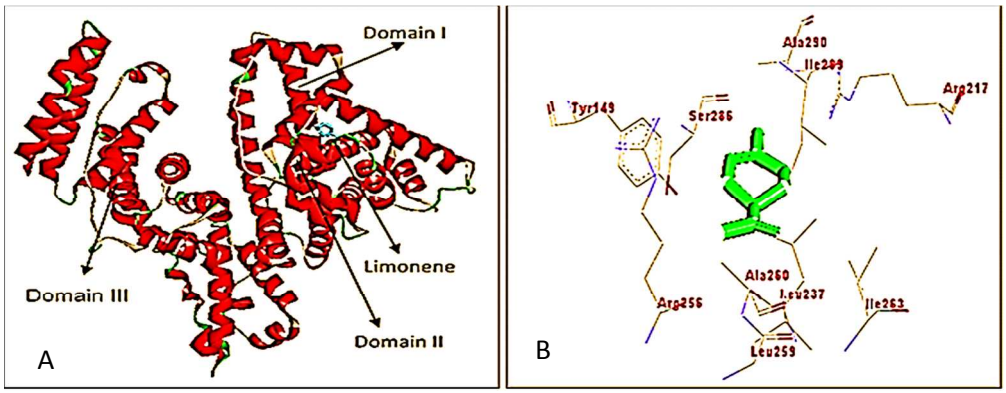

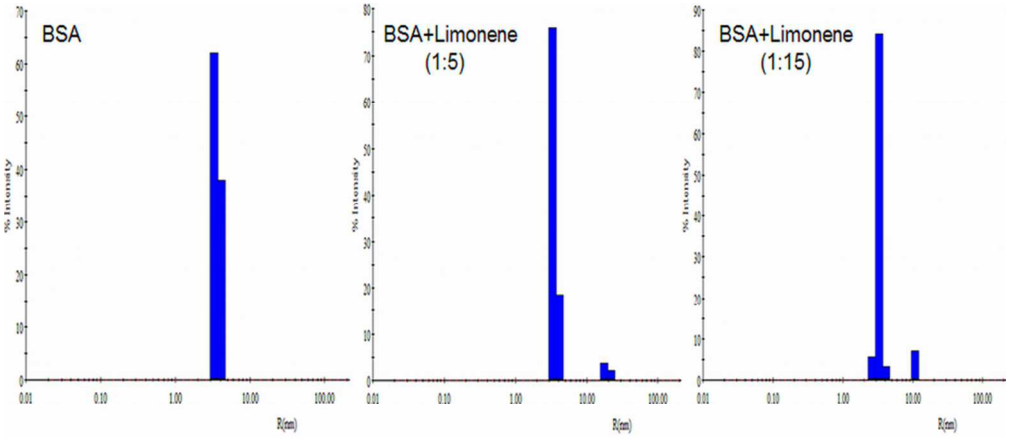


Supplementary figure 1. DLS pattern of BSA-limonene interaction showing Rh distributions.

40x20mm (600 x 600 DPI)

Mechanistic insight into the BSA-limonene interaction: biophysical and molecular docking approach.